

## RESEARCH ARTICLE

# Estimation of colour volumes as concave hypervolumes using $\alpha$ -shapes

Hugo Gruson 

CEFE, Univ Montpellier, CNRS, Univ Paul Valéry Montpellier 3, EPHE, IRD, Montpellier, France

## Correspondence

Hugo Gruson

Email: hugo.gruson@normalesup.org

Handling Editor: Sean Rands

## Abstract

1. Organisms often display multiple colour patches and for many analyses, it may be useful to take into account all these patches at the same time, and reconstruct the colour volume of the organisms. Stoddard and Prum (2008, *The American Naturalist*, 171, 755) proposed to use convex hulls to reconstruct the colour volume of a species. Convex hull volume has since then often been used as an index of colourfulness, and the intersection of multiple convex hulls is used to study the colour similarity between two objects.
2. In this article, I outline the limitations of convex hulls in this context. In particular, multiple studies have reported that the convex hull overestimates the actual colour volume. I argued for the use of a more general tool, developed as a more flexible extension of the convex hulls:  $\alpha$ -shapes. Depending on the parameter  $\alpha$ ,  $\alpha$ -shapes can reconstruct concave (i.e. non-convex) volumes with voids or pockets that are better suited for the estimation of colour volumes.
3. To determine the optimal value of the parameter  $\alpha$ , I point out two expected properties of multidimensional trait spaces, which translate into two conditions providing a lower and upper bound on  $\alpha$ , and I propose technical tools to identify the  $\alpha$  value satisfying these two conditions. Using colour data from the whole bird community from the biological station of the Nouragues, French Guiana, I show that using  $\alpha$ -shapes rather than convex hulls results in possibly major differences in the estimation of the colour volume.
4. I discuss possible future developments of this new framework in both colour science and other areas of ecology dealing with multidimensional trait spaces, such as community ecology where  $\alpha$ -shape volumes could serve as a replacement for the functional richness FRic, or morphometrics.

## KEYWORDS

colour volume, colourfulness, concave hull, convex hull, functional richness, hyper volumes, morphospace,  $\alpha$ -shapes

## 1 | INTRODUCTION

Colour is a communication channel widespread among a wide range of taxa (Bradbury & Vehrencamp, 2011; Schaefer, 2010). Many

organisms do not display a single colour but rather an assemblage of colours on their body and it may be relevant to study all colour patches at the same time, instead of running independent analyses for each patch (Endler & Mielke, 2005). To study all the different colours in a single integrative analysis, Stoddard and Prum (2008) defined the *colour volume*, which they described as a measure of colour

The peer review history for this article is available at <https://publons.com/publon/10.1111/2041-210X.13398>

diversity of an individual or a species. This colour volume was computed by building the minimal **convex set** (terms in bold are defined in the glossary at the end of this manuscript), also called **convex hull**, containing all data points (Figure 1a). An intuitive definition of a convex set is that it must contain all line segments connecting any pair of points. In 2011, this metric was extended by Stoddard and Stevens to compare colours between entire organisms or objects (such as eggs from nest parasites vs. hosts) using vision models by computing the overlap between the convex hulls of the two objects.

The convex hull may seem like an obvious choice for this task. It is commonly used in many areas of biological sciences to build a volume from a set of data points because it has many computational (efficient algorithms such as those presented in Barber, Dobkin, & Huhdanpaa, 1996; Chan, 1996; Graham, 1972; Kirkpatrick & Seidel, 1986) and mathematical (unicity, conservation of convexity by projection or intersection, etc.) benefits. It is, for example, known as a measure for functional richness (often denoted **FRic**) in community ecology (Cornwell, Schwillk, & Ackerly, 2006; Villéger, Mason, & Mouillot, 2008), as a tool to evaluate species distributions (Burgman & Fox, 2003), body mass from skeletons in palaeontology (Sellers et al., 2012) or morphospaces (Kotrc & Knoll, 2015; Nordén et al., 2019). However, no study has hitherto discussed the biological and evolutionary relevance of convex volumes to describe the colour space that can be produced by a taxon. Convexity is indeed a strong mathematical property that has been criticized in other areas of ecology (Burgman & Fox, 2003; Galton & Duckham, 2006). On the contrary, if we relax the convexity hypothesis, we get concave volumes which are defined as the absence of convexity and do therefore not make any assumption on the nature of the data. Some criticisms against convex hulls for colour volumes already emerged because it could not properly fit datasets that were obviously concave, as reported by Delhey (2015) in his study on Australian birds colour, and often led to an overestimation of the actual volume. Additionally, as reported previously (Blonder, Lamanna, Violle, & Enquist, 2014; Delhey, 2015; Eliason, Shawkey, & Clarke, 2016; Kotrc & Knoll, 2015; Maia & White, 2018; Renoult, Kelber, & Schaefer, 2017; Stournaras et al., 2013; Worton, 1995), convex polygons (such as the convex hull) are strongly influenced by outliers, which can cause errors in

the estimation of the volume or the shape. It is worth noticing that the original authors (Stoddard & Prum, 2008) already highlighted these weaknesses in their founding article and alerted readers about the possible dangers in the interpretation of colour volumes, when used with no additional metrics.

In spite of those criticisms, no alternative has been proposed yet and convex hull volumes are still routinely used in colour science (Bukovac et al., 2017; Burd, Stayton, Shrestha, & Dyer, 2014; Dalrymple et al., 2018; Delhey, 2015; Doutrelant et al., 2016; Enbody, Lantz, & Karubian, 2017; Galván, Negro, Rodríguez, & Carrascal, 2013; Hanley, Stoddard, Cassey, & Brennan, 2013; Langmore et al., 2011; Merwin, Smith, & Seeholzer, 2020; Muchhala, Johnsen, & Smith, 2014; Ödeen, Pruett-Jones, Driskell, Armenta, & Håstad, 2012; Ornelas, González, Hernández-Baños, & García-Moreno, 2016; Pérez i de Lanuza, Font, & Monterde, 2013; Prum, LaFountain, Berro, Stoddard, & Frank, 2012; Renoult, Courtiol, & Schaefer, 2013; Spottiswoode & Stevens, 2012; Stoddard, 2012; Stoddard & Prum, 2011; Stournaras et al., 2013; White, Dalrymple, Herberstein, & Kemp, 2017).

In this article, I propose the use of a new mathematical tool to estimate colour volumes and colour volumes overlap, which works even for non-convex set of points:  $\alpha$ -shapes (Edelsbrunner, Kirkpatrick, & Seidel, 1983; Edelsbrunner & Mücke, 1994).  $\alpha$ -Shapes are a generalization of convex hulls that aim at proposing a mathematical definition to the intuitive concept of shape of a set of points. They also present multiple benefits compared to other concave hulls (discussed in more details later on): (a) they can work in an arbitrary number of dimensions, and efficient algorithms exist for either two- or three-dimensional data (algorithmic time complexity of  $O(n \log n)$  in 2D; Edelsbrunner et al., 1983; Edelsbrunner & Mücke, 1994), (b) they are already used in other areas of ecology and evolution (Brassey & Gardiner, 2015; Burgman & Fox, 2003), which means there are readily available and well-tested tools to compute them (such as Matlab *Matlab*2018 or Pateiro-López & Rodríguez-Casal, 2010; Lafarge & Pateiro-López, 2017 in R) and (c) when  $\alpha$  is large enough, the  $\alpha$ -shape algorithm gives the same output as the convex hull (Edelsbrunner et al., 1983), which means both the current Stoddard and Prum (2011)'s and the new approach described here can be thought of as using  $\alpha$ -shapes, only with different choices of  $\alpha$ .

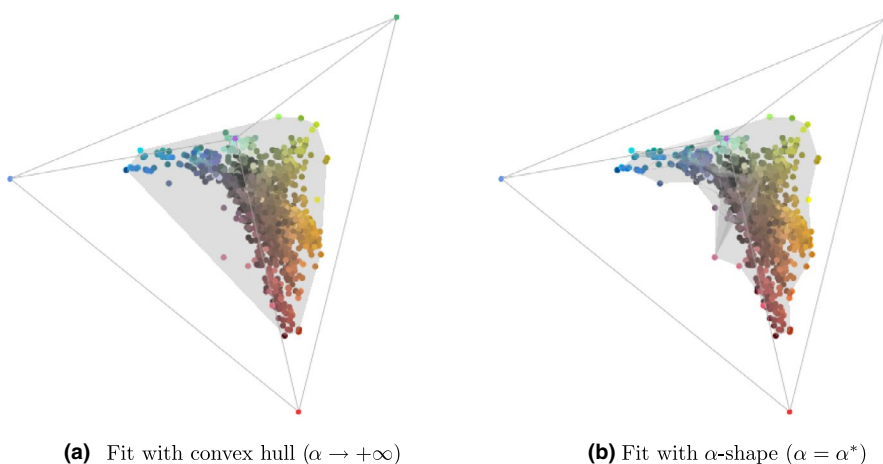


**FIGURE 1** Comparison of the fits with (a) a convex hull (plotted with the `vol()` function from the R package `pavo`) and (b) an  $\alpha$ -shape with the optimal  $\alpha^*$  value determined in this study, plotted with the new `tetrashape()` function available in ESM. Each point is the colour of one patch from birds living in the Nouragues rainforest, in French Guiana, represented in the colour space of an average VS bird species, under ideal illumination. The colour of the points corresponds to the colour of the data points as seen in human colour vision

## 2 | MATERIALS AND METHODS

### 2.1 | Definition of $\alpha$ -shapes and algorithm

An intuitive way of thinking about an  $\alpha$ -shape in 2D is by the 'eraser tool' analogy (Edelsbrunner et al., 1983; Edelsbrunner & Mücke, 1994): imagine your data points shown in an image editing software and with the eraser tool set to a particular size (circle of radius  $\alpha$ ) and you clear everything you can without erasing any of the data points. What remains is known as an  $\alpha$ -hull, which is related but not identical to the  $\alpha$ -shape (see Figure 2). Where the  $\alpha$ -hull generated by the eraser method has curved edges, the  $\alpha$ -shape has straight edges, formed by directly linking points along the edge of the  $\alpha$ -hull.

In practice, calculation of the  $\alpha$ -shape works differently from the eraser tool analogy and is instead based on the Delaunay triangulation. A Delaunay triangulation is a one specific way of joining points using non-intersecting triangles (2D), tetrahedra (3D) or more generally simplices (the general term for triangles, tetrahedra and their equivalents in any dimension). In the actual calculation, instead of doing the erasing and then joining up the points, we join the points first and then do some erasing. The Delaunay triangulation is special in that a circle containing the points of each triangle—its

circumcircle—does not contain any other points. This property has equivalents in the 3D, 4D and higher dimensional cases, and it is what is exploited in the algorithm used to calculate the  $\alpha$ -shape. If we have triangle from a Delaunay triangulation and its circumcircle has a radius greater than  $\alpha$ , then we know that there is a large enough circular space absent points to fit the 'eraser tool'. This means that the triangle cannot be on the 'inside' of the  $\alpha$ -shape, and we remove it (Edelsbrunner et al., 1983; Edelsbrunner & Mücke, 1994). The algorithm for the computation of  $\alpha$ -shapes is thus as follows:

1. Compute the Delaunay triangulation of the set of points.
2. Remove all Delaunay triangles (simplices) whose circumcircle (circumsphere) has radius  $\geq \alpha$ .

### 2.2 | Example data: Bird colours from the Nouragues rainforest

The present article uses two types of data to demonstrate the strengths of  $\alpha$ -shapes over convex hulls: (a) simulated data and (b) empirical data of quantum catches from the entire bird community from the Nouragues rainforest, in French Guiana, as seen by a

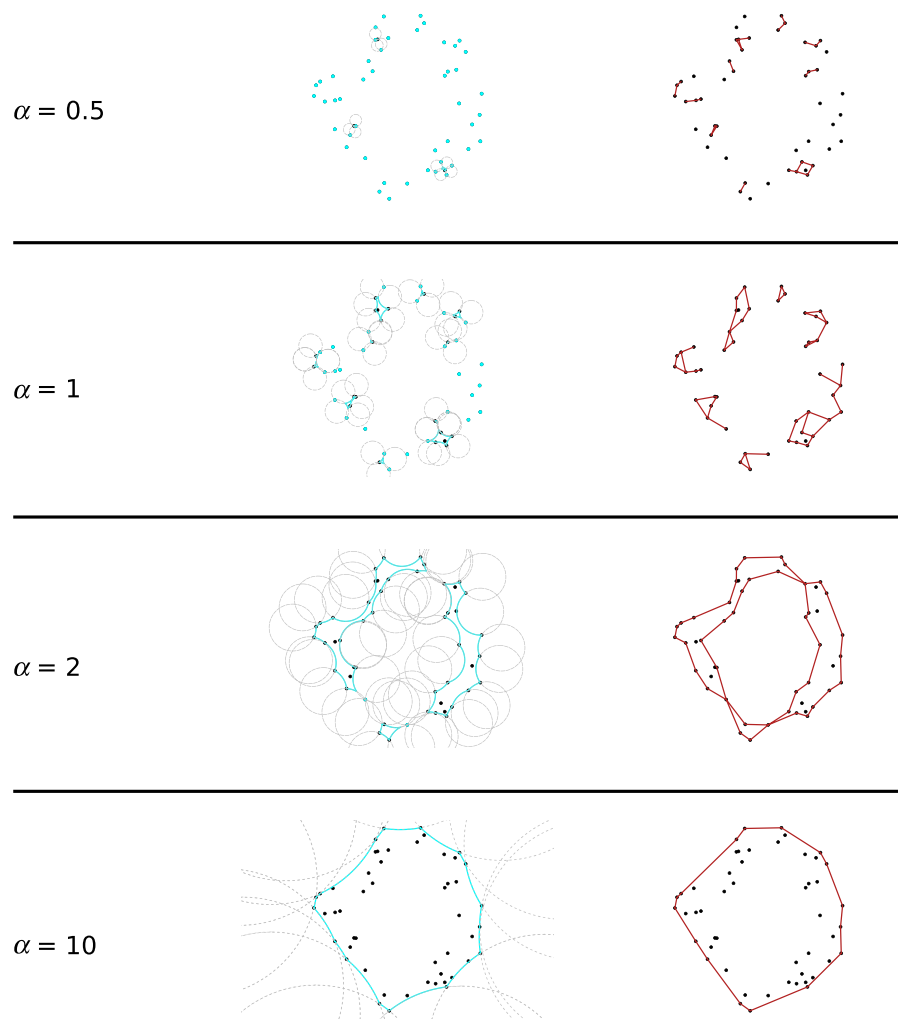


**FIGURE 2** Illustration of  $\alpha$ -hull (cyan; left panel) and  $\alpha$ -shape (red; right panel) for different  $\alpha$  values on a fictive dataset. The  $\alpha$ -hull is what remains once circles of radius  $\alpha$  have been dug out without removing any points ('eraser intuition'). The  $\alpha$ -shape can be derived from the  $\alpha$ -hull by drawing straight lines instead of curves between the vertices (' $\alpha$ -neighbours')

UVS bird viewer under ideal illumination (constant reflectance for all wavelengths). Reflectance measurements were collected by Doris Gomez using a deuterium-halogen light source, a bifurcated optic probe at 45° and a spectrophotometer calibrated relative to a dark reference and a white spectralon standard to ensure that measurements were independent of the light source and spectrometer used.

## 2.3 | Characteristics of colour spaces

Although the method presented here can be generalized to more general multidimensional niches and trait spaces, I will focus mostly on the case of colour spaces, which present several characteristics which simplify slightly the problem at hand.

Colour spaces are multidimensional polygons that contain all colours that an organism can perceive. The most common colour spaces are chromaticity diagrams. Chromaticity diagrams are regular  $(n - 1)$ -simplices where  $n$  is the number of photoreceptors from the species of interest. For example, in the case of trichomat species, the chromaticity diagram is Maxwell's triangle and in the case tetrachromat species, it is a tetrahedron (Endler & Mielke, 2005; Stoddard & Prum, 2008).

The coordinates of the chromaticity diagram vertices and thus the total possible volume have no real biological significance and are based on arbitrary conventions (Renoult et al., 2017). Because of this, independently derived visual models may have different vertices coordinates and total possible volume. For example, for tetrachromatic chromaticity diagrams (represented in a tetrahedron), which are used for bird vision, two systems of vertices coordinates leading to two different total possible volumes coexist in the literature: the one from Kelber, Vorobyev, and Osorio (2003), with total volume of  $1/3$  and the one from Endler and Mielke (2005) and Stoddard and Prum (2008), with total volume of  $\sqrt{3}/8 \approx 0.2165$ . For this reason, colour volume should always be reported as a proportion of the total possible volume (using, e.g., `rel.c.vol` column from `pavo`'s R package `summary.colospace()` output) instead of an absolute value.

Alternatively, articles should always report the total possible volume alongside the realized colour volume.

Reporting colour volumes as proportion of the total possible volume also allows to compare it between different organisms, even when they have different numbers of photoreceptors (e.g. colour volume in the trichromatic human colour space versus colour volume in the tetrachromatic bird colour space). On the opposite, comparing volumes across dimensions for multidimensional niches or trait spaces in the general case (not colour spaces) does not make sense.

Alternatively, depending on the biological question, it may make more sense to report colour volume as a proportion of the maximum theoretical colour volume given a visual system and illuminant. Because of the overlap in the photoreceptor sensitivity profiles, it may be biologically impossible to have data points in corners of the chromaticity space (because the case where a single photoreceptor is excited never happens), as illustrated in Figure 3. I provide code to compute this maximal theoretical colour volume and to plot it in the R package `pavo` (Maia, Gruson, Endler, & White, 2019).

Another property of chromaticity diagrams simplifies the exploration of  $\alpha$ -shapes in the present study: chromaticity diagrams are isotropic, which means all directions have the same properties and distance unit. On the opposite, general multidimensional trait spaces used in functional ecology may be anisotropic (e.g. a 2D space with home range and longevity as axes). In this case, a distance of one unit does not have the same meaning depending on the direction. I discuss later in the article how this issue can be mitigated.

## 2.4 | Implementation of $\alpha$ -shapes in colour analysis toolbox `pavo`

I have developed a series of scripts available in supplementary data to easily compute and plot colour volumes with  $\alpha$ -shapes in R (R Core Team, 2019). The  $\alpha$ -shape computation itself is performed thanks to existing R packages (Lafarge & Pateiro-López, 2017; Pateiro-López

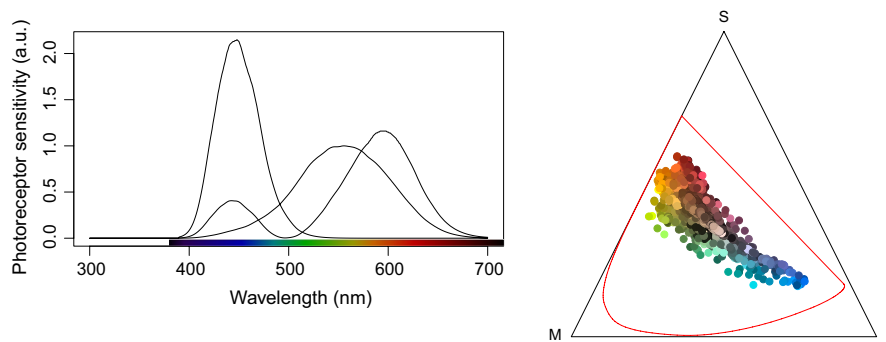


**FIGURE 3** Illustration of how overlap in photoreceptor sensitivity prevents the exploration of the full chromaticity diagram. Left panel: standard human photoreceptor sensitivities, with the bar on the x-axis showing to which colour each wavelength maps. Right panel: Nouragues natural reserve data as seen by a standard human, under ideal illumination (colours as viewed in the human visual system). The chromaticity diagram boundaries are drawn in black (Maxwell's triangle) and the boundaries of the possible colours given the visual system and illuminant are drawn in red. The black and red polygons differ because of the overlap in the photoreceptor sensitivities. In this example, the space delimited by the red boundary corresponds to the CIE 1931 XYZ colour space

& Rodríguez-Casal, 2010). R is a free and open-source programming language and widely used in ecology and evolution, making it a good target for large and rapid dissemination of this method. The provided scripts are also readily compatible with the `pavor` package, a widely used toolbox in colour science (Maia, Eliason, Bitton, Doucet, & Shawkey, 2013; Maia et al., 2019), and provide the `tetrashape()` and `tcsshape()` functions as drop-in replacements for `pavo`'s function which plot convex hulls (`vol()` and `tcsvol()`, respectively). These functions alongside a detailed example showing how to use them are available in ESM.

### 3 | RESULTS AND DISCUSSION

#### 3.1 | Determination of optimal $\alpha$ -value

Most studies using  $\alpha$ -shapes in other fields do not offer guidance on the choice of the value  $\alpha$  and instead recommend the choice is made based on a posteriori visual evaluation of the fit. But for colour volumes (and more generally, for multidimensional niches or trait spaces), there is no theoretical reason to prefer one fit compared to the other (as the general shape of the colour volume is not known) and the a posteriori visual evaluation entirely relies on the user subjective judgement, possibly resulting in biased choices that would better conform to their predictions and expectations.

On the contrary, we want to define an optimal value of  $\alpha$  based on minimal assumptions about the colour volume. There is no 'magic' value for  $\alpha$  that will work for all datasets and this value can only be defined in the context of a given set on points.

But in all cases, we want to satisfy the two following conditions:

**Condition 1** All data points should contribute to the final volume. In other words, there should be no isolated ( $n - 2$ )-simplex (points and lines in 2D; points, lines and triangles in 3D) because their volume is zero, everything happens as if the related data points were discarded from the estimation of the trait volume.

**Condition 2** The shape should fit the data points as closely as possible (following the parsimony principle). In other words, the volume should be minimized given the data points.

The  $\alpha$ -value which meets these two conditions is the  $\alpha^*$  used in Cholewo and Love (1999) and I use their notation in the rest of this article. It also corresponds to the value returned by the `criticalAlpha()` function in MATLAB2014b (or following versions) when used with the option 'all-points' and the default value to build 2D and 3D  $\alpha$ -shapes with the `alphaShape()` function. I also provide in ESM an R script to compute the 3D  $\alpha$ -shapes matching these two criteria.

However, depending on their biological question, users should feel free to define their own conditions and  $\alpha$ -value if necessary (e.g. new condition: 'the colour volume should have only one component').

#### 3.2 | Comparison of $\alpha$ -shapes versus convex hulls for the computation of the volume

Because the volume of  $\alpha$ -shapes increases with  $\alpha$  (Edelsbrunner et al., 1983), we can deduce that  $\alpha$ -shapes will always result in a lower colour volume than convex hulls (which is the case where  $\alpha \rightarrow +\infty$ ). The difference in the estimation of the volume will depend on the dataset. Unsurprisingly, the effect is larger in dataset with holes or concave datasets.

For example, the colour volume of the Nouragues bird community has large empty areas when fitted by a convex hull (Figure 1), in a very similar fashion to what Delhey (2015) found for the bird community of Australia. These empty areas inflate the colour volume of the Nouragues natural reserve to 25% (relative to the total volume of the tetrahedron). When fitted by an  $\alpha$ -shape with the optimal  $\alpha^*$  parameter ( $\alpha \approx 0.111$  for this example), the resulting colour volume is very different and represents only 8.6% of the total volume of the tetrahedron (Figure 4).

Users should, however, pay attention to the case where they get several distinct components in their colour volumes (as it is the case in Figure 6b for example): in this case, the colour volume will not take into account the distance between the different components. In other words, for relatively small values of  $\alpha$ , you may get the same colour volume for, for example, a blue and red object and a brown and red object, even though brown is closer to red than blue in most visual spaces, as illustrated in Figure S4. This might not be suitable depending on your biological question so you should always proceed with care when you get colour volumes with multiple distinct components. An easy fix to this situation is to increase the value of  $\alpha$  until you get a single component.

#### 3.3 | Effect of subsampling and outliers

Convex hulls have been criticized for being highly sensitive to outliers (Maia & White, 2018; Renoult et al., 2017), and this problem worsens as the number of dimensions of the colour space increases.

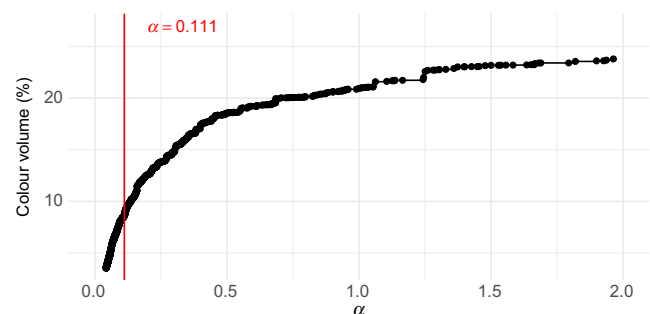


**FIGURE 4** Effect of the value  $\alpha$  on the volume of the resulting  $\alpha$ -shapes, or colour volume, for the Nouragues rainforest bird community. The optimal  $\alpha^*$  ( $\approx 0.111$ ) value for this dataset, identified thanks to the two criteria listed previously, is marked with a red line. The convex hull volume is 25%

For similar reasons to those developed by Reem (2011) about the related mathematical concept of **Voronoi diagrams**,  $\alpha$ -shapes benefit from a relative local stability property. Let us imagine that one data point is removed from the dataset. In the best-case scenario, it is an interior point and this removal does not affect the resulting  $\alpha$ -shape. In the worst-case scenario, this point is a regular vertex linked to the furthest possible  $\alpha$ -neighbours, each lie at a distance  $\alpha$ . This area of the removed Delaunay  $k$ -simplex is then  $\left(\sqrt{k+1} / (k! \sqrt{2^k})\right) \alpha^k$ . We notice that the change in colour volume with the removal of one point increases with  $\alpha$ . Therefore, the change in colour volume with the framework proposed here is smaller than the change with a convex hull ( $\alpha$  large).

For the same reason, measurement errors or noise in the data will only have an effect on the  $\alpha$ -neighbours, and will cause overall an error in the estimation of the volume that directly depends on the value of  $\alpha$ . The error will thus be smaller in the case of  $\alpha$ -shapes than in the case of convex hulls.

This can be verified in Figure 5, where I computed the  $\alpha$ -shape with  $\alpha^*$  and the convex hull volumes after removing randomly 20%, 40% or the outermost 20% (outliers) data points on a subsample of the original

Nouragues dataset.  $\alpha$ -Shapes and convex hulls are affected roughly in the same way when random points are removed. This is to be expected because the chance of removing an interior point is higher for convex hull but the effect will be larger when a non-interior point is removed (as explained in the previous paragraph). On the other hand, when the outermost points (outliers) are removed, the impact on the resulting volume is greater with the convex hull approach.

### 3.4 | Comparison of $\alpha$ -shapes versus convex hulls for the computation of the overlap

One of the criticisms against convex hulls is that they can create spurious overlap values. This is actually due to the fact that convex hulls can include large areas with no data points.  $\alpha$ -Shapes, because they more closely fit the data points (especially if you use the  $\alpha^*$  value recommended in this study), should not suffer as much from this weakness. This difference between convex hulls and  $\alpha$ -shapes is illustrated in a example with simulated data for a trichromat viewer in Figure 6.

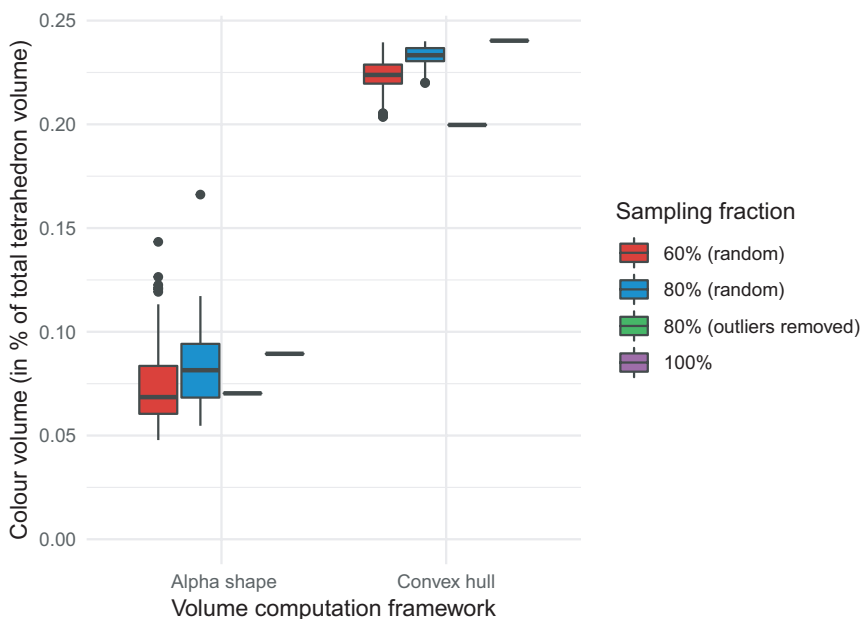


**FIGURE 5** Comparison of the removal of random points or outliers on the resulting volume computed with the  $\alpha$ -shape (and  $\alpha^*$ ) or the convex hull. This analysis was performed on a subset of the Nouragues dataset, and the removal of random points was ran 100 times

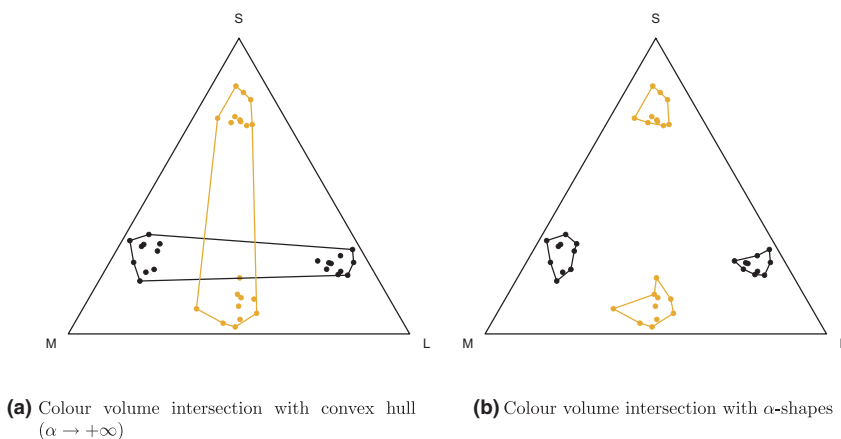


**FIGURE 6** Overlaps of colour volumes for fictive data in the chromaticity diagram of a trichromat, estimated with (a) a convex hull or (b) an  $\alpha$ -shape. Two different fictive species are figured with different colours. The estimation with the convex hull can create spurious non-zero overlap values even in the case when the two species do not share any common colours. This is not the case for  $\alpha$ -shapes



There is currently no exact algorithm to compute the intersection of concave polygons, such as  $\alpha$ -shapes, in an arbitrary number of dimensions (but see `st_intersect()` function from the `sf` R package for 2D; Pebesma, 2018). A computationally efficient method is then to use a Monte Carlo approach, as was done in Stoddard and Prum (2008) and Blonder et al. (2014). An example for  $\alpha$ -shapes in 3D is given in ESM (`overlap3d()`, drop-in replacement for `pavo::voloverlap()`).

### 3.5 | Comparison of $\alpha$ -shapes versus other concave hull fitting methods

$\alpha$ -Shapes have interesting unique properties compared to other types of concave hulls used in the literature and in other areas of ecology and evolution:

- Concaveman, described in Park and Oh (2012), is an algorithm that builds possibly concave hulls by removing edges larger than a given threshold value from the convex hull. However, current implementations only work in 2D (Gombin, Vaidyanathan, & Agafonkin, 2017), which is not suitable for tetrachromat and pentachromat viewers, as well as for its use to describe a multidimensional niche or trait space in a more general case.
- The `hypervolume` R package provides a method based on multi-dimensional kernel density estimation (KDE) to construct possibly concave hypervolumes from data points, even in a high number of dimensions (Blonder et al., 2014; 2018). It has met a large success for the description of multidimensional niches but the probabilistic approach makes it more difficult to formally derive general properties of the niche or the intersection of niches. The KDE and the  $\alpha$ -shape approaches also fundamentally differ in the way extreme points (outliers) are considered. Depending on the parameters, the KDE approach used in the `hypervolume` approach will mainly focus on the areas with high point density and may leave extreme points outside of the niche (depending on the threshold value). On the opposite, the  $\alpha$ -shape approach presented in this article will include all points in the resulting niche. Depending on the biological question, either of these two approaches may be preferred to the other. Interestingly, in high dimensions, the only computationally tractable way to use this KDE method is to use a uniform kernel (i.e. a rectangular function), making the `hypervolume` and the  $\alpha$ -shape approaches highly related from a mathematical point of view (Edelsbrunner, 1995), as detailed in ESM.

### 3.6 | Perspectives: $\alpha$ -shapes in other domains of ecology and evolution

$\alpha$ -shapes could be used in colour science on other spaces than chromaticity diagrams, such as perceptually uniform spaces (Cassey et al., 2008; Pike, 2012b). But they could also be prove valuable in other subfields from ecology and evolution where the

use of convex hulls gives rise to growing criticism. However, caution is required to transpose the approach we describe here. As mentioned before, the colour space is known a priori and is isotropic (i.e. all directions have the same properties). Conversely, in functional ecology or in morphometrics for example, trait spaces may be composed by binary, discrete or continuous traits which means all directions are not equivalent and one unit of dimension does not have the same meaning in every direction. To solve this issue, data must be normalized beforehand, as already reported in previous studies about other types of concaves volumes (Blonder et al., 2014). In these fields, depending on the expected properties of the computed volume (e.g. possibility of gaps or unconnected components) and the biological, the optimal  $\alpha$  value may not be  $\alpha^*$  but the introduction to the mathematical concepts and the code presented here will still surely prove useful.

As of today, the main limitation to use  $\alpha$ -shapes in other fields lies in the fact that current software to compute  $\alpha$ -shapes only work in two or three dimensions, mainly because of a lack of interest (most applications focus on reconstructing 3D objects, such as proteins). However,  $\alpha$ -shapes can easily be generalized to higher dimensions (Edelsbrunner et al., 1983; Edelsbrunner & Mücke, 1994) and the current limitation is purely a computational limitation, with the most computationally intensive step being the Delaunay triangulation (Edelsbrunner & Mücke, 1994). But new, efficient algorithms for the Delaunay triangulation have been developed recently (Hornus & Boissonnat, 2008) and could allow the use of  $\alpha$ -shapes for animals with more than four classes of photoreceptors (Pike, 2012a).

### ACKNOWLEDGEMENTS

I would like to thank Doris Gomez for her valuable comments on an earlier version of this manuscript, the Eco-Evo Mathématiques team at the IBENS for insightful discussions about  $\alpha$ -shapes and multidimensional niches, and Thomas White for his feedback on some of the code developed for this article. I am also extremely grateful to the MEE associate editor who handled this manuscript, as well as Kaspar Delhey and two anonymous reviewers, for their detailed comments that largely contributed to improve this manuscript.

### DATA AVAILABILITY STATEMENT

All data and scripts necessary to reproduce the findings and the figures from this article are available at <https://doi.org/10.5281/zenodo.3747361>.

### ORCID

Hugo Gruson  <https://orcid.org/0000-0002-4094-1476>

### REFERENCES

- Barber, C. B., Dobkin, D. P., & Huhdanpaa, H. (1996). The Quickhull algorithm for convex hulls. *ACM Transactions on Mathematical Software*, 22(4), 469–483. <https://doi.org/10.1145/235815.235821>
- Blonder, B., Lamanna, C., Violle, C., & Enquist, B. J. (2014). The n-dimensional hypervolume. *Global Ecology and Biogeography*, 23(5), 595–609. <https://doi.org/10.1111/geb.12146>

- Blonder, B., Morrow, C. B., Maitner, B., Harris, D. J., Lamanna, C., Violle, C., ... Kerkhoff, A. J. (2018). New approaches for delineating n-dimensional hypervolumes. *Methods in Ecology and Evolution*, 9(2), 305–319. <https://doi.org/10.1111/2041-210X.12865>
- Bradbury, J. W., & Vehrencamp, S. L. (2011). *Principles of animal communication* (2nd ed., p. 697). Sunderland, MA: Sinauer Associates.
- Brassey, C. A., & Gardiner, J. D. (2015). An advanced shape-fitting algorithm applied to quadrupedal mammals: Improving volumetric mass estimates. *Royal Society Open Science*, 2(8), 150302. <https://doi.org/10.1098/rsos.150302>
- Bukovac, Z., Shrestha, M., Garcia, J. E., Burd, M., Dorin, A., & Dyer, A. G. (2017). Why background colour matters to bees and flowers. *Journal of Comparative Physiology A*, 203(5), 369–380. <https://doi.org/10.1007/s00359-017-1175-7>
- Burd, M., Stayton, C. T., Shrestha, M., & Dyer, A. G. (2014). Distinctive convergence in Australian floral colours seen through the eyes of Australian birds. *Proceedings of the Royal Society B*, 281(1781), 20132862. <https://doi.org/10.1098/rspb.2013.2862>
- Burgman, M. A., & Fox, J. C. (2003). Bias in species range estimates from minimum convex polygons: Implications for conservation and options for improved planning. *Animal Conservation*, 6(1), 19–28. <https://doi.org/10.1017/S1367943003003044>
- Cassey, P., Ewen, J. G., Blackburn, T. M., Hauber, M. E., Vorobyev, M., & Marshall, N. J. (2008). Eggshell colour does not predict measures of maternal investment in eggs of Turdus thrushes. *Naturwissenschaften*, 95(8), 713–721. <https://doi.org/10.1007/s00114-008-0376-x>
- Chan, T. M. (1996). Optimal output-sensitive convex hull algorithms in two and three dimensions. *Discrete & Computational Geometry*, 16(4), 361–368. <https://doi.org/10.1007/BF02712873>
- Cholewo, T., & Love, S. (1999). Gamut boundary determination using alpha-shapes. *Color and Imaging Conference, 7th Color and Imaging Conference Final Program and Proceedings*, (5), 200–204. <https://www.ingentaconnect.com/content/ist/cic/1999/00001999/00000001/art00037>
- Cornwell, W. K., Schwikl, D. W., & Ackerly, D. D. (2006). A trait-based test for habitat filtering: Convex hull volume. *Ecology*, 87(6), 1465–1471. [https://doi.org/10.1890/0012-9658\(2006\)87\[1465:ATFHF\]2.0.CO;2](https://doi.org/10.1890/0012-9658(2006)87[1465:ATFHF]2.0.CO;2)
- Dalrymple, R. L., Flores-Moreno, H., Kemp, D. J., White, T. E., Laffan, S. W., Hemmings, F. A., ... Moles, A. T. (2018). Abiotic and biotic predictors of macroecological patterns in bird and butterfly coloration. *Ecological Monographs*, 88(2), 204–224. <https://doi.org/10.1002/ecm.1287>
- Delhey, K. (2015). The colour of an avifauna: A quantitative analysis of the colour of Australian birds. *Scientific Reports*, 5, 18514. <https://doi.org/10.1038/srep18514>
- Doutrelant, C., Paquet, M., Renoult, J. P., Grégoire, A., Crochet, P.-A., & Covas, R. (2016). Worldwide patterns of bird colouration on islands. *Ecology Letters*, 19(5), 537–545. <https://doi.org/10.1111/ele.12588>
- Edelsbrunner, H. (1995). The union of balls and its dual shape. *Discrete & Computational Geometry*, 13(3), 415–440. <https://doi.org/10.1007/BF02574053>
- Edelsbrunner, H., Kirkpatrick, D. G., & Seidel, R. (1983). On the shape of a set of points in the plane. *IEEE Transactions on Information Theory*, 29(4), 551–559. <https://doi.org/10.1109/TIT.1983.1056714>
- Edelsbrunner, H., & Mücke, E. P. (1994). Three-dimensional alpha shapes. *ACM Transactions on Graphics*, 13(1), 43–72. <https://doi.org/10.1145/174462.156635>
- Eliason, C. M., Shawkey, M. D., & Clarke, J. A. (2016). Evolutionary shifts in the melanin based color system of birds. *Evolution*, 70(2), 445–454. <https://doi.org/10.1111/evo.12855>
- Enbody, E. D., Lantz, S. M., & Karubian, J. (2017). Production of plumage ornaments among males and females of two closely related tropical passerine bird species. *Ecology and Evolution*, 7(11), 4024–4034. <https://doi.org/10.1002/ece3.3000>
- Endler, J. A., & Mielke, P. W. (2005). Comparing entire colour patterns as birds see them. *Biological Journal of the Linnean Society*, 86(4), 405–431. <https://doi.org/10.1111/j.1095-8312.2005.00540.x>
- Galton, A., & Duckham, M. (2006). What is the region occupied by a set of points? In M. Raubal, H. J. Miller, A. U. Frank, & M. F. Goodchild (Eds.), *Geographic information science* (pp. 81–98). Lecture Notes in Computer Science. Berlin, Heidelberg: Springer.
- Galván, I., Negro, J. J., Rodríguez, A., & Carrascal, L. M. (2013). On showy dwarfs and sober giants: Body size as a constraint for the evolution of bird plumage colouration. *Acta Ornithologica*, 48(1), 65–80. <https://doi.org/10.3161/000164513X670007>
- Gombin, J., Vaidyanathan, R., & Agafonkin, V. (2017). *concaveman: A very fast 2D concave hull algorithm*. Version 1.0.0. Retrieved from <https://CRAN.R-project.org/package=concaveman>
- Graham, R. L. (1972). An efficient algorithm for determining the convex hull of a finite planar set. *Information Processing Letters*, 1(4), 132–133. [https://doi.org/10.1016/0020-0190\(72\)90045-2](https://doi.org/10.1016/0020-0190(72)90045-2)
- Hanley, D., Stoddard, M. C., Cassey, P., & Brennan, P. L. (2013). Eggshell conspicuousness in ground nesting birds: Do conspicuous eggshells signal nest location to conspecifics? *Avian Biology Research*, 6(2), 147–156. <https://doi.org/10.3184/175815513X13617279883973>
- Hornus, S., & Boissonnat, J.-D. (2008). An efficient implementation of Delaunay triangulations in medium dimensions. Report. INRIA. p. 15. <https://hal.inria.fr/inria-00343188/document>
- Kelber, A., Vorobyev, M., & Osorio, D. (2003). Animal colour vision – Behavioural tests and physiological concepts. *Biological Reviews*, 78(1), 81–118. <https://doi.org/10.1017/S1464793102005985>
- Kirkpatrick, D. G., & Seidel, R. (1986). The ultimate planar convex hull algorithm? *SIAM Journal on Computing*, 15(1), 287–299. <https://doi.org/10.1137/0215021>
- Kotrc, B., & Knoll, A. H. (2015). A morphospace of planktonic marine diatoms. I. Two views of disparity through time. *Paleobiology*, 41(1), 45–67. <https://doi.org/10.1017/pab.2014.4>
- Lafarge, T., & Pateiro-López, B. (2017). *alphashape3d: Implementation of the 3D alpha-shape for the reconstruction of 3D sets from a point cloud*. Version 1.3. Retrieved from <https://CRAN.Rproject.org/package=alphashape3d>
- Langmore, N. E., Stevens, M., Maurer, G., Heinsohn, R., Hall, M. L., Peters, A., & Kilner, R. M. (2011). Visual mimicry of host nestlings by cuckoos. *Proceedings of the Royal Society B: Biological Sciences*, 278(1717), 2455–2463. <https://doi.org/10.1098/rspb.2010.2391>
- Maia, R., Eliason, C. M., Bitton, P.-P., Doucet, S. M., & Shawkey, M. D. (2013). pavo: An R package for the analysis, visualization and organization of spectral data. *Methods in Ecology and Evolution*, 4(10), 906–913. <https://doi.org/10.1111/2041-210X.12069>
- Maia, R., Gruson, H., Endler, J. A., & White, T. E. (2019). pavo 2: New tools for the spectral and spatial analysis of colour in R. *Methods in Ecology and Evolution*, 10(7), 1097–1107. <https://doi.org/10.1111/2041-210X.13174>
- Maia, R., & White, T. E. (2018). Comparing colors using visual models. *Behavioral Ecology*, 29(3), 649–659. <https://doi.org/10.1093/beheco/ary017>
- Matlab. (2018). *Version 2018b*. Natick, Massachusetts: The Mathworks Inc.
- Merwin, J. T., Smith, B. T., & Seeholzer, G. F. (2020). Macroevolutionary bursts and constraints generate a rainbow in a clade of tropical birds. *BMC Evolutionary Biology*, 20(1), 32. <https://doi.org/10.1186/s12862-020-1577-y>
- Muchhala, N., Johnsen, S., & Smith, S. D. (2014). Competition for hummingbird pollination shapes flower color variation in Andean Solanaceae. *Evolution*, 68(8), 2275–2286. <https://doi.org/10.1111/evo.12441>
- Nordén, K. K., Faber, J. W., Babarović, F., Stubbs, T. L., Selly, T., Schiffbauer, J. D., ... Vinther, J. (2019). Melanosome diversity and convergence in the evolution of iridescent avian feathers—Implications for paleocolor reconstruction. *Evolution*, 73(1), 15–27. <https://doi.org/10.1111/evo.13641>
- Ödeen, A., Pruett-Jones, S., Driskell, A. C., Armenta, J. K., & Håstad, O. (2012). Multiple shifts between violet and ultraviolet vision in a



- family of passerine birds with associated changes in plumage coloration. *Proceedings of the Royal Society B: Biological Sciences*, 279(1732), 1269–1276. <https://doi.org/10.1098/rspb.2011.1777>
- Ornelas, J. F., González, C., Hernández-Banós, B. E., & García-Moreno, J. (2016). Molecular and iridescent feather reflectance data reveal recent genetic diversification and phenotypic differentiation in a cloud forest hummingbird. *Ecology and Evolution*, 6(4), 1104–1127. <https://doi.org/10.1002/ece3.1950>
- Park, J.-S., & Oh, S.-J. (2012). A new concave hull algorithm and concaveness measure for n-dimensional datasets. *Journal of Information Science and Engineering*, 28(3), 587–600.
- Pateiro-López, B., & Rodríguez-Casal, A. (2010). Generalizing the convex hull of a sample: The R package alphahull. *Journal of Statistical Software*, 34(1), 1–28. <https://doi.org/10.18637/jss.v034.i05>
- Pebesma, E. (2018). Simple features for R: Standardized support for spatial vector data. *The R Journal*, 10(1), 439–446. Retrieved from <https://journal.r-project.org/archive/2018/RJ-2018-009/index.html>
- Pérez i de Lanuza, G., Font, E., & Monterde, J. L. (2013). Using visual modelling to study the evolution of lizard coloration: Sexual selection drives the evolution of sexual dichromatism in lacertids. *Journal of Evolutionary Biology*, 26(8), 1826–1835. <https://doi.org/10.1111/jeb.12185>
- Pike, T. W. (2012a). Generalised chromaticity diagrams for animals with n-chromatic colour vision. *Journal of Insect Behavior*, 25(3), 277–286. <https://doi.org/10.1007/s10905-011-9296-2>
- Pike, T. W. (2012b). Preserving perceptual distances in chromaticity diagrams. *Behavioral Ecology*, 23(4), 723–728. <https://doi.org/10.1093/beheco/ars018>
- Prum, R. O., LaFountain, A. M., Berro, J., Stoddard, M. C., & Frank, H. A. (2012). Molecular diversity, metabolic transformation, and evolution of carotenoid feather pigments in cotingas (Aves: Cotingidae). *Journal of Comparative Physiology B*, 182(8), 1095–1116. <https://doi.org/10.1007/s00360-012-0677-4>
- R Core Team. (2019). *R: A language and environment for statistical computing*. Version, 3.5. Retrieved from <https://www.r-project.org/>
- Reem, D. (2011). The geometric stability of Voronoi diagrams with respect to small changes of the sites. In *Proceedings of the twenty-seventh annual symposium on computational geometry* (pp. 254–263). Paris, France: SoCG '11ACM. <https://doi.org/10.1145/1998196.1998234>
- Renoult, J. P., Courtiol, A., & Schaefer, H. M. (2013). A novel framework to study colour signalling to multiple species. *Functional Ecology*, 27(3), 718–729. <https://doi.org/10.1111/1365-2435.12086>
- Renoult, J. P., Kelber, A., & Schaefer, H. M. (2017). Colour spaces in ecology and evolutionary biology. *Biological Reviews*, 92(1), 292–315. <https://doi.org/10.1111/brv.12230>
- Schaefer, H. M. (2010). Visual communication: Evolution, ecology, and functional mechanisms. In P. Kappeler (Ed.), *Animal behaviour: Evolution and mechanisms* (pp. 3–28). Berlin, Heidelberg: Springer. [https://doi.org/10.1007/978-3-642-02624-9\\_1](https://doi.org/10.1007/978-3-642-02624-9_1)
- Sellers, W. I., Hepworth-Bell, J., Falkingham, P. L., Bates, K. T., Brassey, C. A., Egerton, V. M., & Manning, P. L. (2012). Minimum convex hull mass estimations of complete mounted skeletons. *Biology Letters*, 8(5), 842–845. <https://doi.org/10.1098/rsbl.2012.0263>
- Spottiswoode, C. N., & Stevens, M. (2012). Host-parasite arms races and rapid changes in bird egg appearance. *The American Naturalist*, 179(5), 633–648. <https://doi.org/10.1086/665031>
- Stoddard, M. C. (2012). Mimicry and masquerade from the avian visual perspective. *Current Zoology*, 58(4), 630–648. <https://doi.org/10.1093/czoolo/58.4.630>
- Stoddard, M. C., & Prum, R. O. (2008). Evolution of avian plumage color in a tetrahedral color space: A phylogenetic analysis of New World buntings. *The American Naturalist*, 171(6), 755–776. <https://doi.org/10.1086/587526>
- Stoddard, M. C., & Prum, R. O. (2011). How colorful are birds? Evolution of the avian plumage color gamut. *Behavioral Ecology*, 22(5), 1042–1052. <https://doi.org/10.1093/beheco/arr088>
- Stoddard, M. C., & Stevens, M. (2011). Avian vision and the evolution of egg color mimicry in the common cuckoo. *Evolution*, 65(7), 2004–2013. <https://doi.org/10.1111/j.1558-5646.2011.01262.x>
- Stournaras, K. E., Lo, E., Böhning-Gaese, K., Cazetta, E., Matthias Dehling, D., Schleuning, M., ... Martin Schaefer, H. (2013). How colorful are fruits? Limited color diversity in fleshy fruits on local and global scales. *New Phytologist*, 198(2), 617–629. <https://doi.org/10.1111/nph.12157>
- Villéger, S., Mason, N. W. H., & Mouillot, D. (2008). New multidimensional functional diversity indices for a multifaceted framework in functional ecology. *Ecology*, 89(8), 2290–2301. <https://doi.org/10.1890/07-1206.1>
- White, T. E., Dalrymple, R. L., Herberstein, M. E., & Kemp, D. J. (2017). The perceptual similarity of orb-spider prey lures and flower colours. *Evolutionary Ecology*, 31(1), 1–20. <https://doi.org/10.1007/s10682-016-9876-x>
- Worton, B. J. (1995). A convex hull-based estimator of home-range size. *Biometrics*, 51(4), 1206. <https://doi.org/10.2307/2533254>

## SUPPORTING INFORMATION

Additional supporting information may be found online in the Supporting Information section.

**How to cite this article:** Gruson H. Estimation of colour volumes as concave hypervolumes using  $\alpha$ -shapes. *Methods Ecol Evol*. 2020;11:955–963. <https://doi.org/10.1111/2041-210X.13398>